# Phosphorylation of Apolipoprotein-E at an Atypical Protein Kinase CK2 PSD/E Site in Vitro†

Mark Raftery,‡ Ross Campbell,§ Elias N. Glaros,§ Kerry-Anne Rye,|| Glenda M. Halliday,⊥ Wendy Jessup,§ and Brett Garner*,§

*Bioanalytical Mass Spectrometry Facility, Centre for Vascular Research, University of New South Wales, Sydney NSW 2052, Australia, Heart Research Institute, Camperdown NSW 2050, Australia, and Prince of Wales Medical Research Institute, University of New South Wales, Sydney NSW 2052, Australia*

*Received March 2, 2005; Revised Manuscript Received March 31, 2005*

ABSTRACT: Apolipoprotein-E (apoE) plays an important role in neuronal lipid transport and is thought to stabilize microtubules by preventing tau hyperphosphorylation. ApoE is also associated with insoluble amyloid detected in Alzheimer disease brain lesions. The apoE C-terminal shares several physicochemical features with α-synuclein, another neuronal apolipoprotein-like protein. α-Synuclein is phosphorylated by protein kinase CK2 (CK2) at an atypical PSD/E motif in vivo and in vitro. We identified a similar PSD/E motif in apoE and therefore investigated its potential phosphorylation by CK2 in vitro. When a [$^{32}$P]-labeling approach was used, CK2 readily phosphorylated purified human apoE as well as recombinant forms of human apoE3 and apoE4. Using liquid chromatography mass spectrometry techniques, we mapped the major apoE CK2 phosphorylation site to Ser296 within the apoE PSD/E motif. We also found that apoE potently activated CK2 as demonstrated by increased CK2$\beta$ subunit autophosphorylation and by increased phosphorylation of tau when the latter was added to the kinase reaction mixtures. Other proteins such as apolipoprotein A-I and albumin did not effectively activate CK2. The phosphorylation of apoE by CK2 as well as the activation of CK2 by apoE may be relevant in vivo where apoE, CK2, and tau are co-localized with additional CK2 targets on neuronal microtubules.

Apolipoprotein-E (apoE)[1] is a ∼34 kDa glycoprotein that exists in humans as one of three common isoforms, E2, E3, or E4, which differ in their Cys/Arg composition at residues 112 and 158 (*1*). ApoE contains a 22 kDa N-terminal 4-helix bundle (NT, 1−191) and a 12 kDa C-terminal (CT, 216−299) that is predicted to contain three amphipathic α-helices (*2, 3*). These domains are linked by a region that contains an O-linked oligosaccharide at Thr194, and a thrombin cleavage site is situated between Arg191 and Ala192 (*4, 5*). The NT domain contains a polybasic low-density lipoprotein (LDL) receptor-binding region (140−150) and the sites giving rise to the three human isoforms (*6*). The CT domain contains the major lipid-binding region (223−266) (*3*). Both domains contain heparin-binding sites, residues 142−147 in the NT and within residues 243−272 in the CT. CT residues 268−289 are proposed to play a crucial role in apoE self-association (*7, 8*).

ApoE plays a role in plasma lipid transport and lipid redistribution during neuronal repair and development (*6, 9*). ApoE-containing lipoproteins promote neurite outgrowth, and this activity is thought to result from both lipid supply and direct effects on microtubule assembly (*10, 11*). ApoE interacts with the microtubule-associated protein tau, preventing its hyperphosphorylation and thereby stabilizing microtubules (*12*). Compared to the APOE3 genotype, APOE4 is associated with increased risk and earlier onset of sporadic and late-onset familial Alzheimer's disease (AD) (*13*). Multiple mechanisms appear to underlie the association of APOE genotype with AD. It has been suggested that apoE3 interacts with amyloid-$\beta$ peptide (A$\beta$) thereby facilitating amyloid clearance from the CNS (see ref *14* and references therein), while apoE4 can potentially promote amyloid formation and neurotoxicity (*15, 16*). The apoE4 isoform also promotes A$\beta$-induced neurotoxicity via lysosomal destabilization (*17*). In addition, compared to apoE3, apoE4 is thought to less effectively prevent the hyperphosphorylation of tau which contributes to the formation of paired helical filaments and insoluble neurofibrillary tangles found in AD brain lesions (*12, 18*).

In a previous study of apoE expression during apoptosis and senescence, we provided evidence for apoE phosphorylation in vivo using a [$^{32}$P] metabolic labeling/immunoprecipitation approach (*19*). We recognized that apoE CT structure was predicted to be similar to the apolipoprotein-

† This work was supported by the Australian National Health and Medical Research Council and the Australian Research Council.

* To whom correspondence should be addressed: phone, 61-2-9385 8730; fax, 61-2-9385 1389; e-mail, brett.garner@unsw.edu.au.

‡ Bioanalytical Mass Spectrometry Facility, University of New South Wales.

§ Centre for Vascular Research, University of New South Wales.

|| Heart Research Institute.

⊥ Prince of Wales Medical Research Institute, University of New South Wales.

[1] Abbreviations: A$\beta$, amyloid beta peptide; AD, Alzheimer's disease; apoA-I, apolipoprotein-A-I.; apoE, apolipoprotein-E; BSA, bovine serum albumin; CK2, protein kinase CK2 (previously casein kinase 2); CSF, cerebrospinal fluid; CT, carboxy terminal; HDL, high-density lipoprotein; NT, amino terminal; POPC; 1-palmitoyl-2-oleylphosphatydilcholine.

10.1021/bi0504052 CCC: $30.25 
Published on Web 04/21/2005

like structure (specifically the amphipathic α-helical content) of α-synuclein, another protein that plays a role in neurobiology and in a diverse group of neurodegenerative disorders that have been referred to as synucleinopathies (*20*). The synucleinopathies share a common pathologic lesion containing insoluble α-synuclein aggregates which are thought to contribute to degeneration in vulnerable cell populations (*21*).

Despite the absence of significant sequence homology, the apoE CT domain is similar to α-synuclein in several physicochemical and functional aspects, including the capacity to self-associate in the absence of lipid, the promotion of self-association by heparin/heparan sulfate structures, the increased expression of both proteins during apoptosis, and their targeting to the nucleus under certain circumstances (*19, 20, 22*−*24*). In addition, proteolytic processing of both α-synuclein and apoE accelerates their aggregation in vivo, and this is thought to contribute to neurodegeneration (*22, 25, 26*).

Recent studies have shown that α-synuclein is phosphorylated by protein kinase CK2 (CK2) at an atypical PSD/E site (Ser129) which resides in the carboxy terminus (*27*). CK2-mediated phosphorylation of α-synuclein Ser129 stimulates aggregation and filament formation in vitro and in vivo (*28*). Phosphorylation of α-synuclein at Ser129 may therefore accelerate lesion formation in Parkinson's disease (*28*). Comparisons of the apoE CT and α-synuclein amino acid sequence indicate that apoE also contains an atypical PSD/E CK2 phosphorylation site (Ser296) close to the carboxy terminus. The aim of the present study was to investigate the phosphorylation of apoE by CK2 in vitro and to map potential phosphorylation sites.

## EXPERIMENTAL PROCEDURES

*Materials.* Human apoE3 (cat. no. A50120H) and rabbit apoE (cat. no. A95199H) were from Biodesign (Saco, ME). Purified (>90% pure) rat liver CK2, recombinant 441-tau, bovine serum albumin (BSA), cholesterol, 1-palmitoyl-2-oleylphosphatydilcholine (POPC), and cholate were from Sigma (St. Louis, MO). [$\gamma$-$^{32}$P]ATP specific activity of 10 mCi/mL was from PerkinElmer (Rowville, Vic, Australia). All other solvents and reagents were obtained in the highest purity available from commercial suppliers.

*Isolation of ApoA-I.* Human apoA-I was purified from pooled human plasma-derived HDL by sequential ultracentrifugation ($1.07 < d < 1.21$ g/mL) (*29*). The HDL were delipidated, and apoA-I was isolated by anion exchange fast-protein liquid chromatography (*30*). The isolated apoA-I was detected as a single band following SDS−PAGE and Coomassie staining.

*Preparation of Recombinant ApoE3 and ApoE4.* Recombinant human apoE3 and apoE4 were obtained by overexpression in *Escherichia coli* strain BL21-CodonPlus (Stratagene, La Jolla, CA) using pET32a vectors with thioredoxin as the fusion partner (Novagen, Madison, WI) (*29, 31*). Vectors containing human cDNA for either apoE3 or apoE4 were kindly provided by Dr. Karl Weisgraber, Gladstone Institute of Cardiovascular Disease, University of California, San Francisco, CA. The apoE−thioredoxin complex was obtained by sonicating the cells and removing debris by centrifugation at 32 000 rpm for 20 min using a TLA-100.4 rotor (Beckman, Fullerton, CA). Thioredoxin was cleaved from the apoE with thrombin, and apoE was isolated by gel permeation chromatography on a column of Sephacryl S-300 (Amersham, Piscataway, NJ). The isolated apoE appeared as a single band following SDS−PAGE and silver staining.

*Preparation of Lipidated Recombinant ApoE3.* Complexes of recombinant apoE3, POPC, and cholesterol were prepared using the cholate dialysis method as described previously (*32, 33*). The stoichiometry of POPC/cholesterol/apoE in the purified lipidated apoE complexes was 114.6:13.9:1.0. Quantitation of the lipid and apoE components was based on enzymatic and immunoturbidometric analysis, respectively, using a Cobas Fara autoanalyzer (Roche Diagnostics, Switzerland) as described previously (*34*).

*In Vitro Phosphorylation.* Purified human apoE3 (routinely 200 ng) was mixed with a kinase reaction buffer comprised of 30 mM Tris HCl (pH 7.5), 0.01% Triton X-100, 10 mM 2-mercaptoethanol, 0.2 mM phenylmethanesulfonyl fluoride, 5 $\mu$g/mL leupeptin, 0.4 mM EGTA, 10 mM $MgCl_2$, and 50 $\mu$M [$\gamma^{32}$P]ATP (1 $\mu$Ci) containing 0.7 units (1 unit transfers 1 nmole of phosphate from ATP to casein per minute at pH 7.5 and 37 °C) of CK2 in a final volume of 50 $\mu$L and incubated for 30 min at 30 °C. Reactions were stopped by addition of an equal volume of 2× Laemmli sample buffer and heating at 95 °C for 5 min. The radiolabeled samples were run on 12% polyacrylamide gels and subjected to phosphorimage analysis. Where indicated, the concentration of apoE was varied or replaced with either BSA or apoA-I. In specific experiments, 1 $\mu$g of 441-tau was also added to the reaction mixtures. All experiments were repeated at least twice.

*Western Blotting.* ApoE was detected by western blotting as previously described (*35*). Proteins were mixed with 2× Laemmli sample buffer and run on 12% polyacrylamide−SDS gels using a Mini-Protean II system (BioRad) and subsequently transferred to nitrocellulose membranes. The membranes were incubated for 16 h at 4 °C with a rabbit anti-human apoE polyclonal antibody (cat. no. A 0077, DAKO, Denmark) diluted 1/1000, followed by a 1 h incubation with horseradish peroxidase-conjugated goat anti-rabbit IgG antibody (cat. no. P0448, DAKO). Blots were developed by using enhanced chemiluminescence, and the membranes were exposed to X-ray film, developed, and scanned and signal intensity was quantified using NIH Image 1.62 software (*35*).

*Mass Spectrometry.* Coomassie-stained gel bands were incubated with $NH_4HCO_3/CH_3CN$ (1:1, 10 mM) until colorless (~2−4 h), then $CH_3CN$ (2 × 50 $\mu$L, 10 min), and dried under vacuum (SpeedVac, Savant, Farmingdale, NY). Trypsin (100 ng) in $NH_4HCO_3$ (10 mM, 25 $\mu$L) was added, and the solution was incubated at 37 °C for 14 h. The gel pieces were washed with $H_2O$ (0.1% formic acid, 50 $\mu$L) and $H_2O/CH_3CN$ (1:1) (0.1% formic acid, 50 $\mu$L) for 15 min, and the combined extracts were dried and peptides dissolved in $H_2O$ (0.1% formic acid, 20 $\mu$L).

Digest peptides were separated by nano-LC using a Cap-LC autosampler system (Waters, Milford, MA). Samples (5 $\mu$L) were concentrated and desalted onto a micro C18 precolumn (500 m × 2 mm, Michrom Bioresources, Auburn, CA) with $H_2O/CH_3CN$ (98:2, 0.1% formic acid) at 20 $\mu$L/min. After a 4 min wash, the precolumn was automatically switched (Valco 10 port valve, Houston, TX) into line with a fritless nano column manufactured according to Gatlin (*36*).

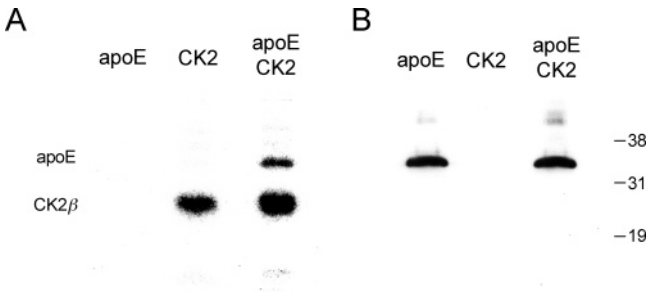


FIGURE 1: Human apoE is phosphorylated by CK2. Purified human apoE3 (100 ng) was incubated with 0.5 unit of CK2 in the presence of 1 $\mu$Ci of [$\gamma$-$^{32}$P]ATP for 30 min in a final volume of 50 $\mu$L of reaction buffer (see Experimental Procedures for details). Five microliter aliquots of the reaction mixtures were separated by PAGE and subjected to (A) phosphorimage analysis and the gels subsequently transferred to nitrocellulose membranes and (B) probed for apoE by western blotting. Position of MW markers are shown with values in kDa.

Peptides were eluted using a linear gradient of $H_2O/CH_3CN$ (95:5, 0.1% formic acid) to $H_2O/CH_3CN$ (40:60, 0.1% formic acid) at 200 nL/min over 30 min. The precolumn was connected via a fused silica capillary (10 cm, 25 $\mu$m) to a low volume tee (Upchurch Scientific) where HV (2600 V) was applied and the column tip positioned 1 cm from the Z-spray inlet of an Ultima API hybrid QTof tandem mass spectrometer (Micromass, Manchester, UK). Positive ions were generated by electrospray and the QTof operated in data dependent acquisition mode (DDA). A TOFMS survey scan was acquired (*m*/*z* 350−1700, 1 s), and the three largest multiply charged ions (counts > 20) were sequentially selected by Q1 for MS-MS analysis. Argon was used as collision gas and an optimum collision energy chosen (based on charge state and mass). Tandem mass spectra were accumulated for up to 6 s (*m*/*z* 50−2000). A processing script generated data suitable for submission to the database search program (Mascot, Matrix Science, London, U.K.). High scores indicated a likely match. Spectra were also interpreted manually to derive amino acids sequences and phosphorylation sites as described previously (*37*).

*In Silico Analysis.* The human apoE amino acid sequence was subjected to in silico analysis using web-based computer algorithms to predict the presence of potential phosphorylation sites (http://www.cbs.dtu.dk/services/netphos) and X-P-S-D/E-X homologous sequence identities (http://www.ncbi.nlm.nih.gov/BLAST) for comparison with the human apoE and α-synuclein PSD/E motifs.

## RESULTS AND DISCUSSION

To assess the possible phosphorylation of apoE by CK2, we treated purified human apoE3 with CK2 in the presence of [$\gamma$-$^{32}$P]ATP. Phosphorimage analysis of the products after separation by PAGE revealed two phosphorylated proteins: the CK2$\beta$ subunit at $M_r$ 26 kDa and apoE at 35 kDa (Figure 1A). To confirm that the 35 kDa band was apoE, proteins from the gels were transferred to nitrocellulose after phosphorimage analysis and probed for apoE by western blotting (Figure 1B). The phosphorylated 35 kDa protein was clearly identified as apoE. ApoE contains six classic consensus sequence motifs (S/T-X-X-D/E) for phosphorylation by CK2, at Thr residues 8, 42, and 67 and Ser residues 76, 129, and 263. We also detected an additional atypical P-S-D/E site with similarities to a known CK2 phosphorylation site within human α-synuclein (Ser129 and Ser296 for α-synuclein and apoE, respectively). To determine the major CK2 phosphorylation site in apoE, we prepared phosphorylated apoE as above (with nonradioactive ATP) and subsequently analyzed for apoE phosphopeptides using LC−MS after tryptic digestion.

ApoE appeared as a doublet with a $M_r$ apoE of ~35 kDa after SDS−PAGE and Coomassie staining (data not shown). After excision, destaining, and in-gel digestion, peptides were separated by nanoLC and analyzed by tandem MS. Both the doublet bands contained sequence specific apoE tryptic peptides with ~50% amino acid sequence coverage. A doubly charged peptide with *m*/*z* 810.85 was identified in both digests, and based on interpretation of the tandem mass spectra and Mascot searches, this peptide was identified as apoE 284−299. An additional peptide with *m*/*z* 850.82 eluting 20 s before apoE 284−299 was detected in the digest of the lower band of the doublet. The mass of this peptide corresponded to the expected mass of phosphorylated apoE 283−299 (+ *m*/*z* 80) (*38*). Sequence specific ions in the tandem mass spectra of both precursors allowed the location of the phosphorylation to be deduced (Figure 2). The partial amino acid sequence AAVGTSAAPV was readily identified from the nonphosphorylated precursor from a series of y-type ions (*m*/*z* 810.85, Figure 2B). A similar series of ions were observed in the tandem mass spectrum of the phosphorylated precursor (*m*/*z* 850.82, Figure 2A). All sequence ions from the phosphorylated precursor show initial loss of $H_3PO_4$ (*m*/*z* 98), forming dehydroalanine, a common and characteristic observation in low-energy collisionally activated tandem mass spectra of phosphopeptides containing phosphoserine (*37*). The amino acid sequence AAVGTSAAPV was also deduced based on the fragment ion pattern in the tandem mass spectrum of phosphorylated precursor ion. The two fragment ions at *m*/*z* 976.29 and *m*/*z* 889.3 correspond to the loss of Ser290. These ions would not be present if Ser290 was phosphorylated. On the basis of the observed fragmentation ions in both tandem mass spectra, it is most likely that phosphorylation occurred specifically at Ser296. This indicates that apoE Ser296 is the preferred site for CK2 phosphorylation. Of potential significance, this site is within the same carboxy terminal PSD/E motif that is phosphorylated by CK2 in α-synuclein (*27*, *28*).

Because there are isoform specific effects of apoE4 in neurodegenerative processes (*39*), the phosphorylation of recombinant human apoE3 and apoE4 was also assessed. In agreement with the data derived from purified human apoE3, CK2 phosphorylated recombinant apoE3 (Figure 3). Furthermore, both apoE3 and E4 isoforms were phosphorylated with equal efficiency (Figure 3). Analysis of the apoE carboxy terminal amino acid sequence in a variety of mammalian species indicated that the region was conserved among humans and nonhuman primates (Table 1). The PSD/E motif was also present in other mammals (e.g., pig and cow) but was absent in the rabbit and rodents (Table 1). To assess the potential phosphorylation of additional residues by CK2, we used purified rabbit apoE as a [$^{32}$P] acceptor. The rabbit apoE was purified using the same methods as for the human apoE3, and both proteins were derived from the same commercial supplier. Rabbit apoE shares 67% amino acid sequence homology with human apoE3 (identities =

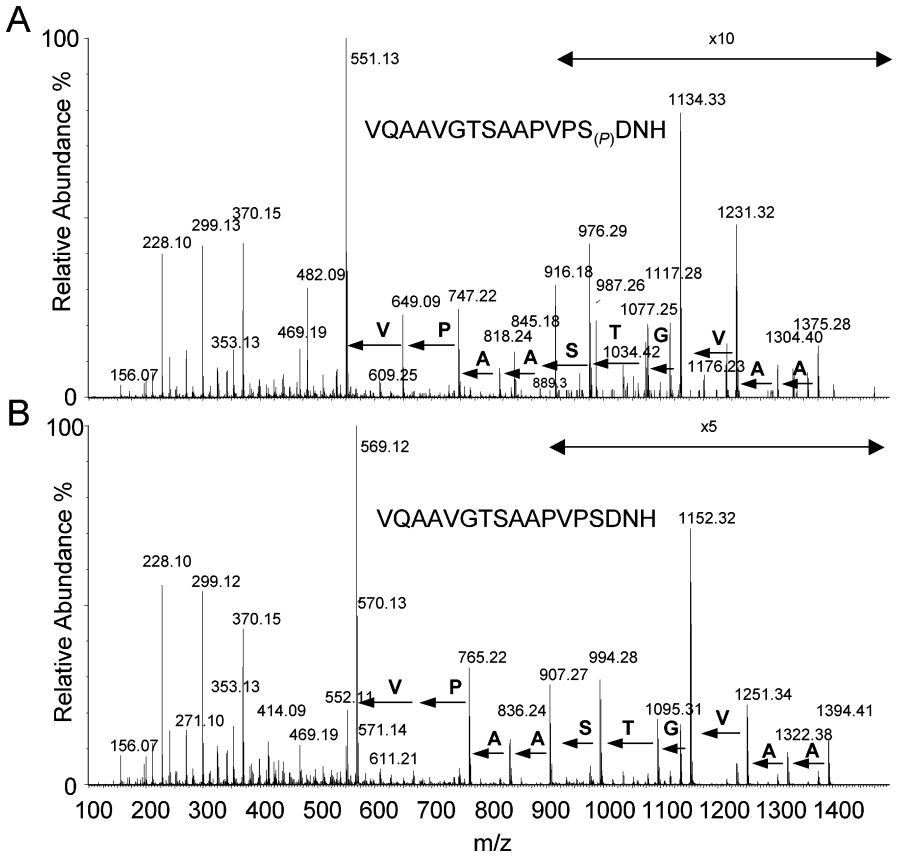


FIGURE 2: ApoE Ser296 is the primary CK2 phosphorylation site. Phosphorylated (A) and nonphosphorylated (B) purified human apoE3 was subjected to in-gel tryptic digestion, and the resulting peptides were subjected to analysis by LC-MS/MS (as described in Experimental Procedures). One predominant phosphopeptide was detected, and MS/MS analysis revealed a single phosphorylated residue at Ser296 (A).

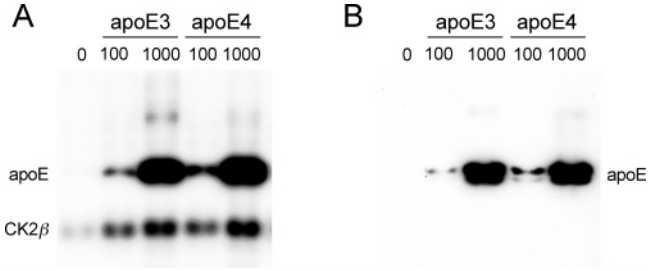


FIGURE 3: Recombinant human apoE3 and apoE4 are equally phosphorylated by CK2. Recombinant human apoE3 and apoE4 were expressed in *E. coli*, purified (as described in Experimental Procedures), and incubated at concentrations of 100 and 1000 ng per tube with 0.5 unit of CK2 in the presence of 1 $\mu$Ci of [$\gamma$-$^{32}$P]-ATP and analyzed by PAGE with subsequent phosphorimage analysis (A) and western blotting (B). Five microliter aliquots of the reaction mixtures were separated by PAGE and subjected to (A) phosphorimage analysis, and the gels were subsequently transferred to nitrocellulose membranes and (B) probed for apoE by western blotting.

215/317 (67%), positives = 245/317 (76%)) and contains eight consensus sequence motifs (S/T-X-X-D/E) for phosphorylation by CK2, four of which are identical to those predicted in the human apoE3 sequence (data not shown). While phosphorylated rabbit apoE was detectable, the level of [$^{32}$P] incorporation was very low compared to parallel incubations with human apoE3 (Figure 4A). Increasing the amount of rabbit apoE in the reaction mixtures did not increase phosphorylation (Figure 4A). These data are consistent with our mass spectrometry analysis and indicate that Ser296 (which is not present in rabbit apoE) is the major site for CK2-mediated phosphorylation in human apoE.

Table 1: Comparison of Mammalian ApoE Carboxy Terminal Amino Acid Sequences

| Species | ApoE C-terminal sequence |
|---|---|
| Human (and primates[a]) | . . . PV**PSD**NH-COOH |
| Pig | . . . SA**PSD**NQ-COOH |
| Cow | . . . SP**PSE**NH-COOH |
| Rabbit | . . . AA**P**I**E**NQ-COOH |
| Mouse/Rat | . . . PVAQ**D**NQ-COOH |

[a] Orangutan, gorilla, chimpanzee, gibbon, and baboon.

In the experiments described above (with the notable exception of those using rabbit apoE), we noticed that the presence of apoE in the reaction mixtures promoted CK2$\beta$ autophosphorylation. The impact of apoE on CK2$\beta$ autophosphorylation appeared to be saturated when apoE was present at levels greater than approximately 250 ng per tube (i.e., 5 $\mu$g/mL, Figure 4A). To further investigate the potential activation of CK2, we used apoE at concentrations ranging from 10 to 1000 ng per tube. ApoE dose-dependently stimulated CK2$\beta$ autophosphorylation (Figure 4B). Even at the lowest apoE concentration used (0.2 $\mu$g/mL), an increase in CK2$\beta$ autophosphorylation was detectable (Figure 4B). This is potentially important as apoE and CK2 are co-localized with neuronal microtubules (*40*−*42*). Microtubule-associated CK2 phosphorylates neuronal specific $\beta$III tubulin and several microtubule-associated proteins (MAPs), including MAP1B, MAP1A, and tau (*43*−*46*). The phosphorylation of these proteins by CK2 promotes microtubule formation

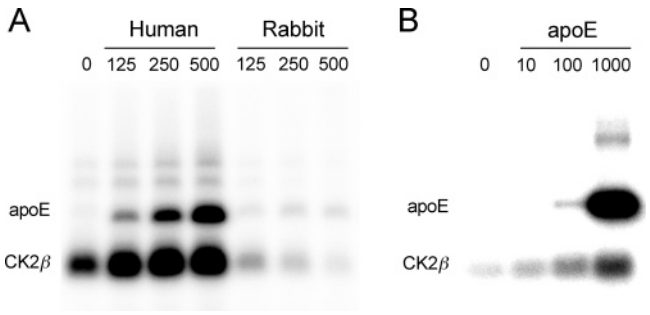


FIGURE 4: Rabbit apoE is not an efficient substrate for or activator of CK2. Purified human apoE3 or rabbit apoE (both used at 125, 250, and 500 ng per tube) was incubated with 0.5 unit of CK2 in the presence of 1 $\mu$Ci of [$\gamma$-$^{32}$P]ATP for 30 min in a final volume of 50 $\mu$L of reaction buffer (see Experimental Procedures for details). Five microliter aliquots of the reaction mixtures were separated by PAGE and subjected to phosphorimage analysis (A). Additional apoE dose dependence data investigating the effect of human apoE3 on CK2$\beta$ autophosphorylation are shown using purified apoE3 at 10, 100, and 1000 ng per tube (B).

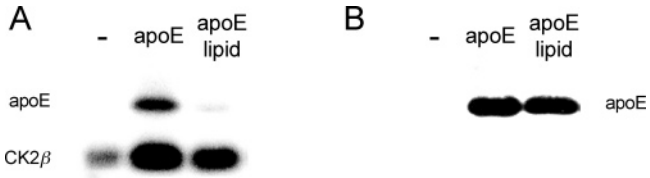


FIGURE 5: Lipidated recombinant human apoE3 is not efficiently phosphorylated by CK2. Recombinant human apoE3 was lipidated with POPC and cholesterol; the complexes were purified (as described in Experimental Procedures), incubated at a concentration of 200 ng apoE per tube with 0.5 unit of CK2 in the presence of 1 $\mu$Ci of [$\gamma$-$^{32}$P]ATP, and analyzed by PAGE with subsequent phosphorimage analysis (A) and western blotting (B). Phosphorylation of lipidated apoE (apoE lipid) was compared to parallel incubations containing no apoE (-) or lipid-free apoE (apoE).

in neuritogenesis (*46*). It is therefore possible that apoE could facilitate neuritogenesis through modulation of CK2 activity.

It is unlikely that apoE bound to microtubules in the cytoplasm is in the form of a lipoprotein complex (*47*); however, it is clear that the majority of apoE in cerebrospinal fluid and plasma is lipidated (*48*). ApoE binds to lipid through the CT domain, and it was therefore of interest to assess the potential for CK2 to phosphorylate lipidated apoE. Figure 5 shows that when apoE was complexed with POPC and cholesterol it was no longer efficiently phosphorylated by CK2. This implies that apoE CT structure is profoundly altered when it is lipidated or that lipid binding close to Ser296 sterically hinders the interaction with CK2. Lipidated apoE also stimulated CK2 autophosphorylation (Figure 5A) which suggests that an interaction between the apoE NT domain and CK2 may be responsible for CK2 activation.

While apoE is thought to inhibit tau hyperphosphorylation (e.g., by binding to and protecting tau from interacting with GSK3$\beta$), our in vitro data indicate that apoE can promote CK2 activity and could thereby potentially stimulate phosphorylation of CK2 targets including tau. We therefore conducted a series of in vitro experiments to assess the potential modulation of CK2-mediated tau phosphorylation by apoE. Confirming previous data (*46*), CK2 stimulated tau phosphorylation (Figure 6A). The predominant phosphorylated tau was present with a $M_r$ of 65 kDa, as predicted for the recombinant tau-441 used in this study. An additional band of phosphorylated tau was detected at the top of the

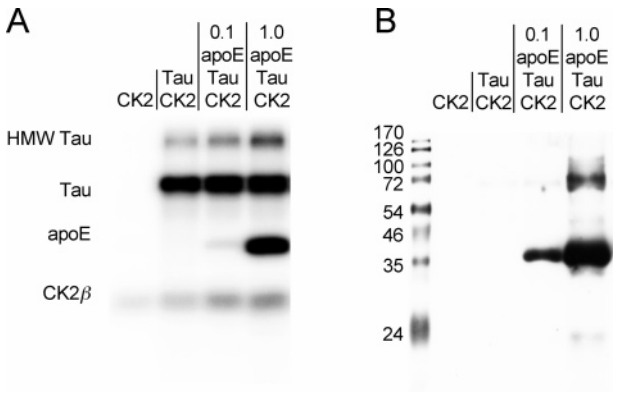


FIGURE 6: Human apoE stimulates CK2$\beta$ autophosphorylation and promotes phosphorylation of HMW tau. Purified human apoE3 (0.1−1.0 $\mu$g) was incubated with 0.5 unit of CK2 in the presence of 1 $\mu$Ci of [$\gamma$-$^{32}$P]ATP for 30 min in a final volume of 50 $\mu$L of reaction buffer with the addition of 1 $\mu$g human r-tau 441. Five microliter aliquots of the reaction mixtures were separated by PAGE and subjected to phosphorimage analysis (A), and the gels were subsequently transferred to nitrocellulose membranes and blotted for apoE (B).

gel with a $M_r$ of approximately 120−180 kDa (Figure 6A). ApoE moderately increased the phosphorylation of the 65 kDa tau band while increasing the formation of high molecular weight (HMW) tau up to approximately 4-fold (Figure 6). Previous studies have shown that hyperphosphorylation of specific residues within the tau microtubule-binding domain promotes its aggregation (reviewed in ref *49*). Our in vitro data imply that microtubule associated apoE could in fact potentiate CK2-mediated tau phosphorylation, although it is not clear if this would have a major impact on tau aggregation in vivo as none of the 14 predicted CK2 phosphorylation sites appear in the tau-441 microtubule-binding domains (which are thought to be important for tau aggregation). Tau is normally phosphorylated in its microtubule-bound state, and it is therefore possible that apoE regulates such "basal" CK2-mediated tau phosphorylation.

Previous studies have shown that polybasic amino acid sequences and synthetic polyamines activate CK2 by binding to a cluster of acidic amino acids in the CK2$\beta$ subunit (*50*). The stimulation of CK2$\beta$ autophosphorylation increases CK2 stability by inhibiting ubiquitin-dependent degradation (*51*). The binding of heparin (a polyanion) to the polybasic residues within potential CK2 activator proteins interferes with the binding of the activator to the CK2 acidic amino acid cluster and thereby inhibits activation through this regulatory domain. Because apoE contains two distinct positively charged heparin-binding domains (*52*), we speculated that the activation of CK2 may be due to specific apoE−CK2 interaction. To investigate the specificity of CK2 activation by apoE, we examined CK2$\beta$ autophosphorylation and the formation of HMW-phosphorylated tau in the presence of either apoE, apoA-I (another amphipathic apolipoprotein that lacks heparin-binding domains), or BSA (a globular protein with no known heparin-binding characteristics).

When expressed on an equal protein mass basis, apoE was clearly the most potent CK2 activator. In contrast to the dose-dependent increase in CK2 activation observed with apoE (Figures 4 and 6), increasing the levels of either BSA or apoA-I in the reaction mixtures did not stimulate CK2

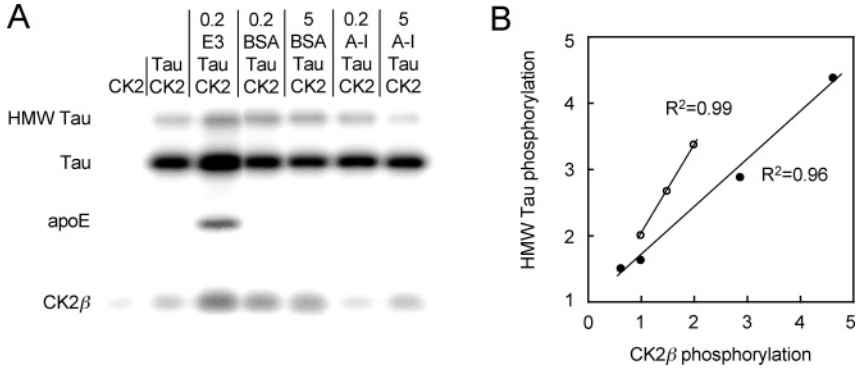


FIGURE 7: Stimulation of CK2 activity and autophosphorylation is specific for apoE. Human apoE3 (0.2 $\mu$g) was incubated with 0.5 unit of CK2 in the presence of 1 $\mu$Ci of [$\gamma$-$^{32}$P]ATP for 30 min in a final volume of 50 $\mu$L of reaction buffer with the addition of 1 $\mu$g human r-tau 441 (A). Either BSA or human apoAI (0.2 and 5 $\mu$g) were also added to tau for comparison. Under these conditions, CK2$\beta$ autophosphorylation was modulated and directly correlated with the level of HMW tau phosphorylation (B). [$^{32}$P] intensity was quantified by NIH image software, and the values are arbitrary with a value of 1 defined as the level of CK2$\beta$ autophosphorylation detected in the presence of tau alone. The solid symbols represent the data derived from Figure 7A (for tau alone or in the presence of 0.2 $\mu$g of apoE, BSA, or apoA-I). The open symbols represent the data derived from Figure 6A (for tau alone or in the presence of 0.1 or 1 $\mu$g of apoE).

Table 2: Identification of PSD/E Motif with Similarity to Human ApoE or α-Synuclein CK2 Phosphorylation Sites[a]

| Protein | PSD/E (CK2) site | Evidence | Swiss Prot |
|---|---|---|---|
| apoE | ...PV**PSD**NH-COOH | *** | P02649 |
| α-Synuclein | ...EM**PSE**EG... | **** | P37840 |
| Furin | ...EC**PSD**S**E**... | **** | P09958 |
| NAP1 (dros.) | ...EV**PSE**Q**E**... | **** | Q24150 |
| IGFBP1 | ...MA**PSE**E**D**... | **** | P08833 |
| PKC-β | ...PP**PSE**G**E**... | *** | P05771 |
| Beta-2 AR | ...TV**PSD**NI... | ** | P07550 |
| CHO Synth 1 | ...KV**PSD**NH... | ** | Q86X52 |
| IL-9 R | ...LV**PSD**NF... | ** | Q01113 |
| GABA-B R2 | ...TV**PSD**NA... | ** | O75899 |
| CD109 | ...LV**PSE**DG... | ** | Q6YHK3 |
| Mint-3 | ...LV**PSE**DL... | ** | O96018 |
| Anillin | ...PM**PSE**EK... | * | Q9NQW6 |
| MG-2 | ...RD**PSE**EH... | * | Q9GZU1 |
| Ataxin-1 | ...TL**PSD**NH... | * | P54253 |

[a] Proteins containing a PSD/E motif that is known to be phosphorylated by CK2 in vivo (****) or in vitro (***) or is flanked by either N, E, or D on the carboxy side and V on the amino side (**) are listed. PSD/E sequences flanked only by N, E, or D on the carboxy side are also shown (*). All of the sequences refer to mammalian proteins except NAP1 which is for the *Drosophila melanogaster* protein. The Swiss Prot accession numbers are listed.

activation above levels observed in the presence of CK2 and tau alone (Figure 7A). At 200 ng per tube, ApoA-I inhibited CK2 activity and CK2-mediated tau phosphorylation. There was a significant correlation between the levels of CK2$\beta$ autophosphorylation observed and the formation of HMW-phosphorylated tau (Figure 7B). The mechanism by which apoE stimulates CK2 activity is not known. Since binding of polybasic residues to the acidic CK2$\beta$ site promotes activity (*50*), one possibility is that the polybasic LDL receptor-binding region of apoE could interact with the acidic regulatory domain of the CK2$\beta$ subunit thereby increasing activity and autophosphorylation. However, unless there are subtle differences in other regions of rabbit apoE that alter the conformation of the LDL receptor-binding domain, the inability of rabbit apoE (which contains an LDL receptor-binding domain identical to human apoE) to stimulate CK2 argues against this idea. Alternatively ,another basic apoE domain could interact with CK2 (*52*). The mechanism underlying CK2 activation by apoE requires further study.

The specific phosphorylation of apoE at Ser296 by CK2 was not predicted using known CK2 motif (S/T-X-X-D/E). It is possible that the Pro residue on the N-terminal side of Ser296 or the close proximity of Ser296 to the carboxy terminal reduces the stringency for CK2 interaction with a consensus motif. ApoE phosphorylation may regulate its proteolytic processing (particularly at the carboxy terminus), intracellular trafficking, or interaction with lipids and proteins. The PSD/E motif appears in several other proteins, at least six of which are phosphorylated by CK2 (Table 2). Future studies should address the potential for CK2 to phosphorylate apoE Ser296 in vivo and the possible influence this has on microtubule function and neurodegeneration.

In conclusion, our studies show that CK2 phosphorylates apoE at an atypical PSD/E motif in vitro. ApoE also stimulates CK2 autophosphorylation, and this can promote phosphorylation of additional substrates such as tau. Because apoE, CK2, and additional CK2 substrate proteins are co-localized on neuronal microtubules, in vivo investigations of apoE phosphorylation and CK2 activation appear to be warranted.

## REFERENCES

1. Rall, S. C., Jr., Weisgraber, K. H., Innerarity, T. L., and Mahley, R. W. (1982) Structural basis for receptor binding heterogeneity of apolipoprotein E from type III hyperlipoproteinemic subjects, *Proc. Natl. Acad. Sci. U.S.A. 79*, 4696−4700.
2. Wilson, C., Wardell, M. R., Weisgraber, K. H., Mahley, R. W., and Agard, D. A. (1991) Three-dimensional structure of the LDL receptor-binding domain of human apolipoprotein E, *Science 252*, 1817−1822.
3. Segrest, J. P., Jones, M. K., De Loof, H., Brouillette, C. G., Venkatachalapathi, Y. V., and Anantharamaiah, G. M. (1992) The amphipathic helix in the exchangeable apolipoproteins: a review of secondary structure and function, *J. Lipid Res. 33*, 141−166.
4. Wernette-Hammond, M. E., Lauer, S. J., Corsini, A., Walker, D., Taylor, J. M., and Rall, S. C., Jr. (1989) Glycosylation of human apolipoprotein E. The carbohydrate attachment site is threonine 194, *J. Biol. Chem. 264*, 9094−9101.

5. Cardin, A. D., Hirose, N., Blankenship, D. T., Jackson, R. L., Harmony, J. A., Sparrow, D. A., and Sparrow, J. T. (1986) Binding of a high reactive heparin to human apolipoprotein E: identification of two heparin-binding domains, *Biochem. Biophys. Res. Commun. 134*, 783−789.
6. Mahley, R. W. (1988) Apolipoprotein E: cholesterol transport protein with expanding role in cell biology, *Science 240*, 622−630.
7. Choy, N., Raussens, V., and Narayanaswami, V. (2003) Intermolecular coiled-coil formation in human apolipoprotein E C-terminal domain, *J. Mol. Biol. 334*, 527−539.
8. Fan, D., Li, Q., Korando, L., Jerome, W. G., and Wang, J. (2004) A monomeric human apolipoprotein E carboxyl-terminal domain, *Biochemistry 43*, 5055−5064.
9. Snipes, G. J., McGuire, C. B., Norden, J. J., and Freeman, J. A. (1986) Nerve injury stimulates the secretion of apolipoprotein E by nonneuronal cells, *Proc. Natl. Acad. Sci. U.S.A. 83*, 1130−1134.
10. Nathan, B. P., Bellosta, S., Sanan, D. A., Weisgraber, K. H., Mahley, R. W., and Pitas, R. E. (1994) Differential effects of apolipoproteins E3 and E4 on neuronal growth in vitro, *Science 264*, 850−852.
11. Nathan, B. P., Chang, K. C., Bellosta, S., Brisch, E., Ge, N., Mahley, R. W., and Pitas, R. E. (1995) The inhibitory effect of apolipoprotein E4 on neurite outgrowth is associated with microtubule depolymerization, *J. Biol. Chem. 270*, 19791−19799.
12. Strittmatter, W. J., Weisgraber, K. H., Goedert, M., Saunders, A. M., Huang, D., Corder, E. H., Dong, L. M., Jakes, R., Alberts, M. J., Gilbert, J. R. et al. (1994) Hypothesis: microtubule instability and paired helical filament formation in the Alzheimer disease brain are related to apolipoprotein E genotype, *Exp. Neurol. 125*, 163−171.
13. Corder, E. H., Saunders, A. M., Strittmatter, W. J., Schmechel, D. E., Gaskell, P. C., Small, G. W., Roses, A. D., Haines, J. L., and Pericak-Vance, M. A. (1993) Gene dose of apolipoprotein E type 4 allele and the risk of Alzheimer's disease in late onset families, *Science 261*, 921−923.
14. Aleshkov, S., Abraham, C. R., and Zannis, V. I. (1997) Interaction of nascent ApoE2, ApoE3, and ApoE4 isoforms expressed in mammalian cells with amyloid peptide beta (1−40). Relevance to Alzheimer's disease, *Biochemistry 36*, 10571−10580.
15. Bales, K. R., Verina, T., Dodel, R. C., Du, Y., Altstiel, L., Bender, M., Hyslop, P., Johnstone, E. M., Little, S. P., Cummins, D. J., Piccardo, P., Ghetti, B., and Paul, S. M. (1997) Lack of apolipoprotein E dramatically reduces amyloid beta-peptide deposition, *Nat. Genet. 17*, 263−264.
16. Holtzman, D. M., Bales, K. R., Tenkova, T., Fagan, A. M., Parsadanian, M., Sartorius, L. J., Mackey, B., Olney, J., McKeel, D., Wozniak, D., and Paul, S. M. (2000) Apolipoprotein E isoform-dependent amyloid deposition and neuritic degeneration in a mouse model of Alzheimer's disease, *Proc. Natl. Acad. Sci. U.S.A. 97*, 2892−2897.
17. Ji, Z. S., Miranda, R. D., Newhouse, Y. M., Weisgraber, K. H., Huang, Y., and Mahley, R. W. (2002) Apolipoprotein E4 potentiates amyloid beta peptide-induced lysosomal leakage and apoptosis in neuronal cells, *J. Biol. Chem. 277*, 21821−21828.
18. Flaherty, D., Lu, Q., Soria, J., and Wood, J. G. (1999) Regulation of tau phosphorylation in microtubule fractions by apolipoprotein E, *J. Neurosci. Res. 56*, 271−274.
19. Quinn, C. M., Kagedal, K., Terman, A., Stroikin, U., Brunk, U. T., Jessup, W., and Garner, B. (2004) Induction of fibroblast apolipoprotein E expression during apoptosis, starvation-induced growth arrest and mitosis, *Biochem. J. 378*, 753−761.
20. Clayton, D. F., and George, J. M. (1998) The synucleins: a family of proteins involved in synaptic function, plasticity, neurodegeneration and disease, *Trends Neurosci. 21*, 249−254.
21. Galvin, J. E., Lee, V. M., and Trojanowski, J. Q. (2001) Synucleinopathies: clinical and pathological implications, *Arch. Neurol. 58*, 186−190.
22. Alves da Costa, C. (2003) Recent advances on alpha-synuclein cell biology: functions and dysfunctions, *Curr. Mol. Med. 3*, 17−24.
23. Davidson, W. S., Jonas, A., Clayton, D. F., and George, J. M. (1998) Stabilization of alpha-synuclein secondary structure upon binding to synthetic membranes, *J. Biol. Chem. 273*, 9443−9449.
24. Bazin, H. G., Marques, M. A., Owens, A. P., III, Linhardt, R. J., and Crutcher, K. A. (2002) Inhibition of apolipoprotein E-related neurotoxicity by glycosaminoglycans and their oligosaccharides, *Biochemistry 41*, 8203−8211.
25. Castano, E. M., Prelli, F., Pras, M., and Frangione, B. (1995) Apolipoprotein E carboxyl-terminal fragments are complexed to amyloids A and L. Implications for amyloidogenesis and Alzheimer's disease, *J. Biol. Chem. 270*, 17610−17615.
26. Huang, Y., Liu, X. Q., Wyss-Coray, T., Brecht, W. J., Sanan, D. A., and Mahley, R. W. (2001) Apolipoprotein E fragments present in Alzheimer's disease brains induce neurofibrillary tangle-like intracellular inclusions in neurons, *Proc. Natl. Acad. Sci. U.S.A. 98*, 8838−8843.
27. Okochi, M., Walter, J., Koyama, A., Nakajo, S., Baba, M., Iwatsubo, T., Meijer, L., Kahle, P. J., and Haass, C. (2000) Constitutive phosphorylation of the Parkinson's disease associated alpha-synuclein, *J. Biol. Chem. 275*, 390−397.
28. Fujiwara, H., Hasegawa, M., Dohmae, N., Kawashima, A., Masliah, E., Goldberg, M. S., Shen, J., Takio, K., and Iwatsubo, T. (2002) alpha-Synuclein is phosphorylated in synucleinopathy lesions, *Nat. Cell Biol. 4*, 160−164.
29. Hime, N. J., Drew, K. J., Hahn, C., Barter, P. J., and Rye, K. A. (2004) Apolipoprotein E enhances hepatic lipase-mediated hydrolysis of reconstituted high-density lipoprotein phospholipid and triacylglycerol in an isoform-dependent manner, *Biochemistry 43*, 12306−12314.
30. Weisweiler, P. (1987) Isolation and quantitation of apolipoproteins A-I and A-II from human high-density lipoproteins by fast-protein liquid chromatography, *Clin. Chim. Acta 169*, 249−254.
31. Morrow, J. A., Arnold, K. S., and Weisgraber, K. H. (1999) Functional characterization of apolipoprotein E isoforms overexpressed in *Escherichia coli*, *Protein Expression Purif. 16*, 224−230.
32. Matz, C. E., and Jonas, A. (1982) Micellar complexes of human apolipoprotein A-I with phosphatidylcholines and cholesterol prepared from cholate-lipid dispersions, *J. Biol. Chem. 257*, 4535−4540.
33. Rye, K. A., and Barter, P. J. (1994) The influence of apolipoproteins on the structure and function of spheroidal, reconstituted high density lipoproteins, *J. Biol. Chem. 269*, 10298−10303.
34. Garner, B., Waldeck, A. R., Witting, P. K., Rye, K. A., and Stocker, R. (1998) Evidence for direct reduction of lipid hydroperoxides by methionine residues of apolipoproteins AI and AII, *J. Biol. Chem. 273*, 6088−6095.
35. Garner, B., Baoutina, A., Dean, R. T., and Jessup, W. (1997) Regulation of serum-induced lipid accumulation in human monocyte-derived macrophages by interferon-gamma. Correlations with apolipoprotein E production, lipoprotein lipase activity and LDL receptor-related protein expression, *Atherosclerosis 128*, 47−58.
36. Gatlin, C. L., Kleemann, G. R., Hays, L. G., Link, A. J., and Yates, J. R., III (1998) Protein identification at the low femtomole level from silver-stained gels using a new fritless electrospray interface for liquid chromatography-microspray and nanospray mass spectrometry, *Anal. Biochem. 263*, 93−101.
37. DeGnore, J. P., and Qin, J. (1998) Fragmentation of phosphopeptides in an ion trap mass spectrometer, *J. Am. Soc. Mass Spectrom. 9*, 1175−1188.
38. McLachlin, D. T., and Chait, B. T. (2001) Analysis of phosphorylated proteins and peptides by mass spectrometry, *Curr. Opin. Chem. Biol. 5*, 591−602.
39. Roses, A. D. (1997) Apolipoprotein E, a gene with complex biological interactions in the aging brain, *Neurobiol. Dis. 4*, 170−185.
40. Serrano, L., Hernandez, M. A., Diaz-Nido, J., and Avila, J. (1989) Association of casein kinase II with microtubules, *Exp. Cell Res. 181*, 263−272.
41. Masliah, E., Iimoto, D. S., Mallory, M., Albright, T., Hansen, L., and Saitoh, T. (1992) Casein kinase II alteration precedes tau accumulation in tangle formation, *Am. J. Pathol. 140*, 263−268.
42. Strittmatter, W. J., Saunders, A. M., Goedert, M., Weisgraber, K. H., Dong, L. M., Jakes, R., Huang, D. Y., Pericak-Vance, M., Schmechel, D., and Roses, A. D. (1994) Isoform-specific interactions of apolipoprotein E with microtubule-associated protein tau: implications for Alzheimer disease, *Proc. Natl. Acad. Sci. U.S.A. 91*, 11183−11186.
43. Diaz-Nido, J., Serrano, L., Mendez, E., and Avila, J. (1988) A casein kinase II-related activity is involved in phosphorylation of microtubule-associated protein MAP-1B during neuroblastoma cell differentiation, *J. Cell Biol. 106*, 2057−2065.
44. Serrano, L., Diaz-Nido, J., Wandosell, F., and Avila, J. (1987) Tubulin phosphorylation by casein kinase II is similar to that found in vivo, *J. Cell Biol. 105*, 1731−1739.

45. Greenwood, J. A., Scott, C. W., Spreen, R. C., Caputo, C. B., and Johnson, G. V. (1994) Casein kinase II preferentially phosphorylates human tau isoforms containing an amino-terminal insert. Identification of threonine 39 as the primary phosphate acceptor, *J. Biol. Chem. 269*, 4373−4380.
46. Avila, J., Ulloa, L., Gonzalez, J., Moreno, F., and Diaz-Nido, J. (1994) Phosphorylation of microtubule-associated proteins by protein kinase CK2 in neuritogenesis, *Cell Mol. Biol. Res. 40*, 573−579.
47. Roses, A. D., Einstein, G., Gilbert, J., Goedert, M., Han, S. H., Huang, D., Hulette, C., Masliah, E., Pericak-Vance, M. A., Saunders, A. M., Schmechel, D. E., Strittmatter, W. J., Weisgraber, K. H., and Xi, P. T. (1996) Morphological, biochemical, and genetic support for an apolipoprotein E effect on microtubular metabolism, *Ann. N. Y. Acad. Sci. 777*, 146−157.
48. Pitas, R. E., Boyles, J. K., Lee, S. H., Hui, D., and Weisgraber, K. H. (1987) Lipoproteins and their receptors in the central nervous system. Characterization of the lipoproteins in cerebrospinal fluid and identification of apolipoprotein B,E(LDL) receptors in the brain, *J. Biol. Chem. 262*, 14352−14360.
49. Buee, L., Bussiere, T., Buee-Scherrer, V., Delacourte, A., and Hof, P. R. (2000) Tau protein isoforms, phosphorylation and role in neurodegenerative disorders, *Brain Res. Rev. 33*, 95−130.
50. Litchfield, D. W. (2003) Protein kinase CK2: structure, regulation and role in cellular decisions of life and death, *Biochem. J. 369*, 1−15.
51. Zhang, C., Vilk, G., Canton, D. A., and Litchfield, D. W. (2002) Phosphorylation regulates the stability of the regulatory CK2beta subunit, *Oncogene 21*, 3754−3764.
52. Saito, H., Dhanasekaran, P., Nguyen, D., Baldwin, F. I., Weisgraber, K. H., Wehrli, S., Phillips, M. C., and Lund-Katz, S. (2003) Characterization of the heparin binding sites in human apolipoprotein E, *J. Biol. Chem. 278*, 14782−14787.

BI0504052